HHS Public Access

Author manuscript

J Neural Transm (Vienna). Author manuscript; available in PMC 2017 February 02.

Published in final edited form as:

J Neural Transm (Vienna). 2017 February ; 124(2): 185–192. doi:10.1007/s00702-016-1635-1.

Clustering of tau-immunoreactive pathology in chronic traumatic encephalopathy

Richard A. Armstrong[1], **Ann C. McKee**[2,3,4], **Victor E. Alvarez**[2,3], and **Nigel J. Cairns**[5]

[1]Vision Sciences, Aston University, Birmingham B4 7ET, UK

[2]VA Boston, Boston, MA 02130, USA

[3]Veterans Affairs Medical Center, Bedford, MA 01730, USA

[4]Department of Neurology and Pathology and Laboratory Medicine, Boston University School of Medicine, Boston, MA 02118, USA

[5]Departments of Neurology and Pathology and Immunology, Washington University School of Medicine, Saint Louis, MO 63110, USA

Abstract

Chronic traumatic encephalopathy (CTE) is a neurodegenerative disorder which may result from repetitive brain injury. A variety of tau-immunoreactive pathologies are present, including neurofibrillary tangles (NFT), neuropil threads (NT), dot-like grains (DLG), astrocytic tangles (AT), and occasional neuritic plaques (NP). In tauopathies, cellular inclusions in the cortex are clustered within specific laminae, the clusters being regularly distributed parallel to the pia mater. To determine whether a similar spatial pattern is present in CTE, clustering of the tau-immunoreactive pathology was studied in the cortex, hippocampus, and dentate gyrus in 11 cases of CTE and 7 cases of Alzheimer's disease neuropathologic change (ADNC) without CTE. In CTE: (1) all aspects of tau-immunoreactive pathology were clustered and the clusters were frequently regularly distributed parallel to the tissue boundary, (2) clustering was similar in two CTE cases with minimal co-pathology compared with cases with associated ADNC or TDP-43 proteinopathy, (3) in a proportion of cortical gyri, estimated cluster size was similar to that of cell columns of the cortico-cortical pathways, and (4) clusters of the tau-immunoreactive pathology were infrequently spatially correlated with blood vessels. The NFT and NP in ADNC without CTE were less frequently randomly or uniformly distributed and more frequently in defined clusters than in CTE. Hence, the spatial pattern of the tau-immunoreactive pathology observed in CTE is typical of the tauopathies but with some distinct differences compared to ADNC alone. The spread of pathogenic tau along anatomical pathways could be a factor in the pathogenesis of the disease.

✉Richard A. Armstrong, R.A.Armstrong@aston.ac.uk.

Compliance with ethical standards

Informed consent was given for the removal of all brain tissue subject to local ethical committee approval and the 1996 Declaration of Helsinki (as modified Edinburgh 2000).

Conflict of interest Other than the stated grants, the authors report no conflicts of interest.

Keywords

Chronic traumatic encephalopathy (CTE); Alzheimer's disease neuropathologic change (ADNC); Tauopathy; Neurofibrillary tangle; Spatial pattern; Spatial correlation

Introduction

Chronic traumatic encephalopathy (CTE) is a neurodegenerative disorder which may result from repetitive brain injury (Geddes et al. 1999; Jordan 2013). It has been recorded in association with a variety of contact sports, including boxing, American football, hockey, and wrestling (Maroon et al. 2015), and has also been reported in military veterans exposed to blast shock waves from explosive devices (Goldstein et al. 2012; McKee et al. 2013, 2014, 2015; Shetty et al. 2014).

Clinical symptoms of CTE include impairment of memory and executive function, behavioural change, and motor dysfunction (Saing et al. 2012). Neuropathologically, CTE cases exhibit reduced gray matter volume in several brain regions, most prominently affecting frontal and anterior temporal lobes and the limbic and striato-nigral systems associated with enlargement of the lateral and third ventricles (McKee et al. 2013, 2016). A spectrum of tau-immunoreactive pathology is present, including neurofibrillary tangles (NFT) (Kieman et al. 2015; McKee et al. 2013), neuropil threads (NT), dot-like grains (DLG) (Armstrong et al. 2016), and astrocytic tangles (AT) (Saing et al. 2012; Stein et al. 2014, 2015), a proportion of the latter resembling thorn-shaped astrocytes observed in other disorders (Armstrong et al. 1999, 2000, 2007a). The isoform profile and phosphorylation state of tau in CTE is similar to that of Alzheimer's disease (AD) (Schmidt et al. 2001) in that both three-repeat (3R) and four-repeat (4R) tau are present in equal ratios. In a proportion of cases, AD neuropathologic change (ADNC), viz., beta-amyloid (Aβ) deposits and neuritic plaques (NP) are present (Graham et al. 1995; Johnson et al. 2012; Stein et al. 2015). In addition, oligodendroglial inclusions (GI) are occasionally present in CTE together with low densities of abnormally enlarged neurons (EN) and vacuolation (Armstrong et al. 2016).

In several tauopathies, e.g., AD (Armstrong 1993a), Pick's disease (PiD) (Armstrong et al. 1998a), CBD (Armstrong and Cairns 2009), and PSP (Armstrong et al. 2007b), tau-immunoreactive inclusions in the cortex are frequently clustered within particular laminae, the clusters being regularly distributed parallel to the pia mater. This clustering pattern could result from the degeneration of neuroanatomical pathways (Armstrong et al. 2001a, b) and a consequence of the 'prion-like' behaviour of pathological tau which spreads among brain regions along anatomical pathways (Goedert et al. 2010; Armstrong and Cairns 2012). Hence, to determine whether similar clustering was present in CTE, the spatial patterns of the tau-immunoreactive pathologies were studied in the cortex and hippocampus in 11 cases of the disease and compared with 7 cases of ADNC without CTE.

Materials and methods

Cases

CTE cases (N = 11, mean age 70 years, SD = 6.42) (Table 1) and ADNC cases not associated with CTE (n = 7, mean age 79 years, SD = 8.83) (Table 1) were obtained from Boston University's CTE centre (VA-BU-CLF Brain Bank). With the exception of one case, a boxer for 26 years (Case C), all individuals with CTE had played American football, career durations being in the range 11–24 years. In addition, all patients had suffered at least one traumatic episode resulting in concussion, some with accompanying loss of consciousness, the majority of cases having experienced multiple episodes of trauma during their careers. All cases were diagnosed according to criteria published by McKee et al. (2016): (1) foci of perivascular NFT, AT, and DLG irregularly distributed in cortex with a predilection for the sulcal depths, (2) NFT in superficial laminae II/III, especially in temporal cortex, and (3) clusters of subpial AT in the cortex as an additional finding. Cases were classified according to the staging system suggested by McKee et al. (2015). Hence, stage 1 cases were characterized by discrete foci of tau pathology in the cerebral cortex most commonly in superior or lateral frontal cortex, stage 2 by multiple foci of tau pathology with evidence of spread to superficial adjacent cortex, the medial temporal lobe being largely spared, stage 3 by substantial spread of pathology in frontal, insular, temporal, and parietal cortex with pathology also affecting the amygdala, hippocampus, and entorhinal cortex, and stage 4 by widespread severe tau pathology affecting most regions of the cerebral cortex and medial temporal lobe with the possible exception of the occipital cortex. The majority of the 11 CTE cases studied were classified as stage 3 or 4. The neuropathology of CTE frequently overlaps with that of common neurodegenerative diseases, such as AD (Maroon et al. 2015) (Table 1). Hence, one case was diagnosed as 'pure' CTE without any associated co-pathology, but the remaining cases exhibited one or more co-pathologies most commonly ADNC (N = 7), primary age-related tauopathy (PART) (N = 2) (Dickson 2009; Crary et al. 2014), hippocampal sclerosis (HS) (N = 4) (Josephs et al. 2006), TDP-43 proteinopathy (N = 8), or argyrophilic grain disease (AGD) (N = 1). National Institute on Aging–Alzheimer's (NIA-AA) association guidelines 'ABC' scores of the CTE cases equated to 'not AD'—'intermediate' level of AD (Hyman et al. 2012). PART is a new neuropathological entity characterized by tau pathology typically in the temporal lobe and is associated with aging independent of amyloid pathology (Dickson 2009; Crary et al. 2014). Hence, cases diagnosed as CTE were also designated as having PART according to the following criteria: (1) a diffuse cerebral atrophy was present most severe in the temporal lobe, (2) NFT were present in the medial temporal lobe, hippocampus, and amygdala, (3) extracellular 'ghost' tangles were present, and (4) sparse diffuse Aβ deposits were present but with few NP (Dickson 2009; Crary et al. 2014).

Neuropathology

These studies were approved by the local Institute Review Board of Boston University and were carried out according to the 1995 Declaration of Helsinki (as modified in Edinburgh, 2000). After death, the next-of-kin provided written consent for brain removal and retention for research studies. Brains were fixed in 10 % neutral buffered formalin for at least 2 weeks, paraffin-embedded, and sections cut at 6 μm. For this study, blocks were taken from:

(1) frontal lobe to study the superior frontal gyrus (SFG) (BA 8, 6), (2) temporal pole (TP) (BA 38, 36), and (3) temporal lobe to study the superior temporal gyrus (STG) (BA 22), (4) entorhinal cortex (EC) (BA 28) at the level of the amygdala, and (5) medial temporal lobe (MTL) to study the subiculum, sector CA1 of the hippocampus (HC), and dentate gyrus (DG). Histologic stains included luxol fast blue in combination with hematoxylin and eosin (LHE) and a modified Bielschowsky silver impregnation. Immunohistochemistry was performed using the following antibodies: Aβ42 (AB5078P; EMD Millipore, Billerica, MA, USA; 1:2000), phosphorylated tau (AT8, Pierce Endogen, Rockford, IL, USA; 1:2000), and phosphorylated TDP-43 (pTDP-43, pS409/410 mouse monoclonal; Cosmo Bio Co Ltd, Tokyo, Japan; 1:2000). Each slide was digitally scanned and subsequently visualized on a PC using the Aperio Image-Scope Software (Leica Biosystems Inc. Buffalo Grove, IL, USA) (Armstrong et al. 2016).

Morphometry

In each cortical gyrus (SFG, TP, STG, and EC), variation in the densities of NFT, NT, DLG, AT, and NP was measured from crest to sulcus parallel to the pia mater, using 250 × 50 μm sample fields arranged contiguously (Armstrong 2003a; Armstrong et al. 2016). Sample fields were superimposed over the image using either the draw or rectangle options (minimum $N = 32$ fields) (Armstrong et al. 2016). The sample fields were located in the upper (approximating to laminae II/III) cortex, the region where the densest tau pathology is observed in CTE (McKee et al. 2014; Armstrong et al. 2016). The short edge of the sample field was orientated parallel with the pia mater and aligned with guidelines drawn on the section. Histological features were also studied in the subiculum ($N = 16$ fields), and in sector CA1 ($N = 16$ fields), the short dimension of the sample field being aligned with the alveus. In the DG, the pathology was quantified in the molecular and granule cell layer ($N = 32$ fields). NFT were present in the cytoplasm of larger cells with a distinct region of haematoxylin-positive cytoplasm, while AT were either distinct cytoplasmic inclusions associated with larger, pale nuclei, or resembled thorn-shaped astrocytes. NT were thread-like structures and some of which were serpiginous, while small circular structures were identified as DLG (Armstrong et al. 2016). To quantify the frequency of the larger blood vessels in CTE, a dashed line was drawn across the image within each sample field parallel to the longer dimension of the field at a random location using the negative pen tool (F3). The frequency of contacts between the dashed lines and all major blood vessel profiles (>10 μm in diameter) within the sample field was recorded (Armstrong 2006a).

Data analysis

To determine the degree of clustering of the tau pathology, the data were analyzed by the spatial pattern analysis (Armstrong 1993b, 1997, 2006b). Departure from a random distribution can be measured by calculating the variance/mean (V/M) ratio of the counts of individual histological features in the contiguous sample fields. If a feature is randomly distributed, the number of samples containing 0, 1, 2, 3 … n, inclusions should correspond to a Poisson distribution and the V/M ratio should approximate to unity. A V/M ratio less than unity indicates a regular distribution and greater than unity a clumped or clustered distribution. If a feature is clustered, the mean size and distribution of the clusters can be obtained from counts of lesions in adjacent sample fields added together successively to

provide data for increasing field sizes, e.g., 200 × 1000 μm, 400 × 1000 μm, 800 × 1000 μm, etc., up to a size limited by the total length of strip sampled. The V/M ratio is calculated at each field size. A V/M peak indicates the presence of regularly spaced clusters and location of the peak indicates mean cluster size, statistical significance of a V/M peak being tested using the 't' distribution (Armstrong 1997). The frequencies of the different clustering patterns were compared using χ^2 contingency tables: (1) between cerebral cortex and subiculum/CA1/DG, (2) among different tau-immunoreactive pathologies, and (3) among cases. Spatial correlations between cluster size of the pathology and frequency of blood vessel contacts were tested using Pearson's correlation coefficient ('r') (Armstrong 2003b).

Results

Figure 1 shows the typical tau-immunoreactive pathology in the TP of a case of CTE (Case A). Clusters of NFT are present in the upper laminae, apparently regularly distributed parallel to the pia mater, and are accompanied by DN and more widely distributed DLG.

Examples of the spatial pattern analysis of the NFT, NT, and DLG in a single region of a case of CTE (Case 6, EC) are shown in Fig. 2. NFT exhibited a V/M peak at a field size of 50 μm, suggesting a regular distribution of clusters of NFT, 50 μm in diameter, distributed parallel to the pia mater. NT exhibited two V/M peaks at field sizes of 100 and 400 μm, suggesting a regular distribution of clusters 50 μm in diameter, aggregated into larger 'superclusters' 400 μm in diameter. The DLG exhibited an increasing V/M with field size without reaching a peak, suggesting a large cluster of DLG, of at least 800 μm in diameter.

The frequency of the different spatial patterns exhibited by the tau-immunoreactive pathology in all CTE regions and cases examined are summarized in Table 2. All features of the pathology were clustered, and in a proportion of regions, the clusters were regularly distributed parallel to the tissue boundary. This spatial pattern was observed in the cortex and in the subiculum/sector CA1/DG, respectively, in 15/42 (36 %) and 13/32 (41 %) analyses of NFT, 26/40 (65 %) and 16/32 (50 %) of NT, 21/43 (49 %) and 22/33 (67 %) of DLG, 7/28 (25 %) and 1/5 (20 %) of AT, and 1/3 (33 %) and 0/1 (0 %) of NP. In a subset of cortical regions, the dimensions of the clusters were in the range 400–800 μm. The frequencies of the different clustering patterns were similar in cerebral cortex and subiculum/CA1/DG. However, there were significant differences among tau pathologies, the NT and DLG exhibiting a greater frequency of regularly distributed clusters than the NFT. Clustering patterns were similar in the two cases with relatively little co-pathology, viz., 'pure' CTE (Case K) and CTE/PART (Case H) compared with all remaining cases and in those cases with and without associated ADNC or TDP-43 proteinopathy. No significant correlations were present between estimated cluster size and disease duration or sporting career length. In addition, there were no significant correlations between cluster sizes of the NFT, NT, and DLG, and CTE stage. However, there were also positive correlations between the cluster size of the pathology and ADNC stage, including NT in the SFG with 'C' (NP) stage ($r = 0.77$, $P < 0.05$) and between DLG in the EC with 'B' (NFT) stage ($r = 0.65$, $P < 0.05$).

Similar spatial patterns of the NFT and NP were observed in the cases of ADNC without CTE (Table 3). Hence, regular spaced clusters of the pathology were observed in the cortex and in the subiculum/sector CA1/DG, respectively, in 22/30 (73 %) and 9/13 (69 %) analyses of NFT and 12/26 (46 %) and 11/20 (55 %) of NP. In addition, there were significant differences in spatial pattern between CTE and ADNC cases with AD cases having a significantly more clustered and CTE more frequent random and uniform distributions of the tau pathology (NFT $\chi^2 = 19.29$, $P > 0.001$; NP $\chi^2 = 9.80$, $P < 0.05$).

Spatial correlations between the densities of tau-immunoreactive pathology and frequency of contacts with major blood vessel profiles in CTE are shown in Table 4. Significant positive spatial correlations with blood vessels were infrequent and present in 14/132 (11 %) of analyses, slightly better than chance, and included either the DN or DLG. Hence, in the majority of regions examined, clustering of the tau-immunoreactive pathology along the gyrus from crest to sulcus was not spatially correlated with the presence of larger blood vessel profiles.

Discussion

Considerable variations in density of the tau-immunoreactive pathology were evident in both CTE and ADNC cases parallel to the tissue boundary in the upper laminae of the cortex and in the subiculum, sector CA1, and DG. Hence, caution is required in the interpretation of results, especially of the CTE case, given the large range of onset and trauma present. Frequently, the pathological features formed clusters, and in a proportion of regions, the clusters were regularly distributed parallel to the pia mater, alveus, or edge of the DG granule cell layer. Similar clustering patterns were observed in ADNC cases without CTE and have also been reported previously in various tauopathies, e.g., NFT in AD (Armstrong 1993a), Pick bodies (PB) in PiD (Armstrong et al. 1998a), neuronal cytoplasmic inclusions (NCI) in CBD (Armstrong and Cairns 2009), and NFT in progressive supranuclear palsy (PSP) (Armstrong et al. 2007b). In addition, the clustering patterns were similar in the two CTE cases with relatively little co-pathology (CTE, CTE/PART), compared with the remaining cases with significant co-pathologies, and in cases with and without associated ADNC or TDP-43 proteinopathy. Hence, regular clustering of the tau-immunoreactive pathology is a feature of CTE and does not appear to depend on the presence of ADNC or TDP-43 co-pathology.

Although the spatial patterns of the tau pathology are similar in CTE cases with and without ADNC, there are differences when compared to ADNC cases without CTE. Hence, NFT and NP were more frequently randomly or uniformly distributed in CTE but present more frequently in well-defined clusters in ADNC. These results suggest that the spatial pattern of the tau pathology in CTE with or without associated ADNC is different to that of ADNC alone. Hence, the presence of CTE makes a significant contribution to the tau pathology of these complex cases.

The previous studies of pathological features in a variety of disorders suggest two explanations for clustering, especially when clusters are regularly spaced. First, Aβ deposits in AD (Armstrong et al. 1998b; Armstrong 2006a) and prion protein (PrP^{sc}) deposits in

Creutzfeldt-Jakob disease (CJD) (Armstrong 2009) are clustered around the major blood vessels. In the cortex, larger arterioles penetrate the pia at regular intervals and then extend vertically through the laminae reaching a maximum density in cortical laminae IV (Bell and Ball 1990) and giving rise to a more or less regular distribution of vessels in the upper laminae (Armstrong 2006a). Clustering of protein deposits around these vessels in AD suggests that an impaired blood brain barrier could be involved in their formation. The present data, however, suggest little overall spatial correlation between the tau pathology and the location of major blood vessel profiles from the crest of the gyrus to the sulcus or in the subiculum, sector CA1, or DG. There may be two explanations for the overall lack of correlation. First, spatial correlations with blood vessels may be specific to certain brain regions. Hence, tau pathology in CTE frequently occurs at higher density in the sulcal depths compared with the crests and upper sides of the gyri (Kieman et al. 2015; McKee et al. 2015; Armstrong et al. 2016). These differences in density are often most marked in frontal cortex, where in some cases, a marked perivascular distribution of NFT and especially AT are present (McKee et al. 2013, 2015). Second, clustering of the tau-immunoreactive pathology around larger blood vessels could be characteristic of the early stages of the pathology in CTE. As the disease develops, however, the pathology spreads to affect capillaries located between the major blood vessel profiles, thus reducing the chance of detecting a spatial correlation due to the abundance of both tau inclusions and capillary profiles (Kawai et al. 1990; Luthert and Williams 1991; Armstrong 2006a, 2009).

Second, as in other tauopathies, clustering of the tau-immunoreactive pathology could be related to the degeneration of specific anatomical pathways. First, in a significant proportion of cortical gyri, the tau pathology, especially the NT and DLG, was present in regularly distributed clusters. Many features of cortical architecture are similarly clustered, e.g., the cells of origin of the cortico-cortical pathways are clustered and occur in bands regularly distributed along the cortex parallel to the pia mater (Hiorns et al. 1991). Second, individual bands of cells associated with the cortico-cortical pathways are approximately 400–1000 μm in width depending on region, and traverse the laminae in columns (Hiorns et al. 1991; De Lacoste and White 1993). In a proportion of gyri, the estimated widths of the clusters of tau pathology, measured parallel to the pia mater, were within this size range. Third, anatomically connected regions exhibited similar regularly distributed patterns of clusters, e.g., in the EC and DG granule cells suggesting an association of the pathology and degeneration of the perforant path (Armstrong et al. 2000). Hence, as in the other tauopathies, clustering of the tau pathology in CTE could be the result of the hypothesized ‘prion-like’ behaviour of tau and it was spread through the brain via cell-to-cell transfer (Goedert et al. 2010). Head trauma could, therefore, initiate damage to blood vessels, especially in sulci, resulting in cellular degeneration close to blood vessels and the formation of foci of pathogenic tau. Pathogenic tau could then spread through the brain along anatomical pathways as hypothesized in other tauopathies (Goedert et al. 2010; Armstrong and Cairns 2012).

In conclusion, the tau-immunoreactive pathology of CTE exhibits a clustering pattern typical of the tauopathies in which the clusters are often regularly distributed parallel to the tissue boundary. Similar types of spatial patterns of NFT and NP were also present in ADNC without CTE, but with some differences when compared with CTE. Although a marked

perivascular distribution of the tau pathology can be observed affecting individual large vessels, especially in sulci; overall, the clustering patterns observed were not spatially related to the larger blood vessel profiles. Hence, local blood vessel damage in CTE could result in the formation of pathologic tau in regions close to blood vessels which then exhibits further neuroanatomical spread to affect a range of brain areas.

Acknowledgments

The authors gratefully acknowledge the use of the resources and facilities at the Edith Nourse Rogers Memorial Veterans Hospital (Bedford, MA, USA). We also gratefully acknowledge the help of all members of the Chronic Traumatic Encephalopathy Program at Boston University School of Medicine, VA Boston, and the Bedford VA, as well as the individuals and families whose participation and contributions made this work possible. This work was supported by the National Institute of Neurological Disorders and Stroke (1U01NS086659-01), Department of Veterans Affairs, the Veterans Affairs Biorepository (CSP 501), the Translational Research Center for Traumatic Brain Injury and Stress Disorders (TRACTS), Veterans Affairs Rehabilitation Research and Development Traumatic Brain Injury Center of Excellence (B6796-C), the National Institute of Aging Boston University Alzheimer's Disease Center (P30AG13846; supplement 0572063345–5). This work was supported by the Charles F. and Joanne Knight Alzheimer's Disease Research Center, Washington University School of Medicine, St. Louis, MO, USA (P50 AG05681 and P01 AG03991 from the National Institute on Aging). This work was also supported by unrestricted gifts from the National Football League, Andlinger Foundation, and WWE.

References

Armstrong RA. Is the clustering of neurofibrillary tangles in Alzheimer's patients related to the cells of origin of specific cortico-cortical projections? Neurosci Lett. 1993a; 160:57–60. [PubMed: 8247334]

Armstrong RA. The usefulness of spatial pattern analysis in understanding the pathogenesis of neurodegenerative disorders, with particular reference to plaque formation in Alzheimer's disease. Neurodegeneration. 1993b; 2:73–80.

Armstrong RA. Analysis of spatial patterns in histological sections of brain tissue. J Neurosci Methods. 1997; 73:141–147. [PubMed: 9196285]

Armstrong RA. Quantifying the pathology of neurodegenerative disorders: quantitative measurements, sampling strategies and data analysis. Histopathology. 2003a; 42:521–529. [PubMed: 12786887]

Armstrong RA. Measuring the degree of spatial correlation between histological features in thin sections of brain tissue. Neuropathology. 2003b; 23:245–253. [PubMed: 14719538]

Armstrong RA. Classic β-amyloid deposits cluster around large diameter blood vessels rather than capillaries in sporadic Alzheimer's disease. Curr Neurovasc Res. 2006a; 3:289–294. [PubMed: 17109624]

Armstrong RA. Measuring the spatial arrangement patterns of pathological lesions in histological sections of brain tissue. J Microsc. 2006b; 221:153–158. [PubMed: 16551275]

Armstrong RA. Spatial correlations between the vacuolation, prion protein (PrPsc) deposits and cerebral blood vessels in sporadic Creutzfeldt–Jacob disease. Curr Neurovasc Res. 2009; 6:239–245. [PubMed: 19807656]

Armstrong RA, Cairns NJ. Clustering and spatial correlations of the neuronal cytoplasmic inclusions, astrocytic plaques and ballooned neurons in corticobasal degeneration. J Neural Transm. 2009; 116:1103–1110. [PubMed: 19551469]

Armstrong RA, Cairns NJ. Different molecular pathologies result in similar spatial patterns of cellular inclusions in neurodegenerative disease: a comparative study of eight disorders. J Neural Transm. 2012; 119:1551–1560. [PubMed: 22678700]

Armstrong RA, Cairns NJ, Lantos PL. Clustering of Pick bodies in Pick's disease. Neurosci Lett. 1998a; 242:81–84. [PubMed: 9533399]

Armstrong RA, Cairns NJ, Lantos PL. Spatial distribution of diffuse, primitive, and classic amyloid-β deposits and blood vessels in the upper laminae of the frontal cortex in Alzheimer's disease. Alzheimer Dis Assoc Disord. 1998b; 2:378–383.

Armstrong RA, Cairns NJ, Lantos PL. Quantification of pathological lesions in the frontal and temporal lobe in ten patients diagnosed with Pick's disease. Acta Neuropathol. 1999; 19:64–70.

Armstrong RA, Cairns NJ, Lantos PL. A quantitative study of the pathological lesions in the neocortex and hippocampus of 12 patients with corticobasal degeneration. Exp Neurol. 2000; 163:348–356. [PubMed: 10833308]

Armstrong RA, Lantos PL, Cairns NJ. The spatial pattern of prion protein deposits in patients with sporadic Creutzfeldt– Jacob disease. Neuropathology. 2001a; 21:19–24. [PubMed: 11304038]

Armstrong RA, Cairns NJ, Lantos PL. What does the study of spatial patterns tell us about the pathogenesis of neurodegenerative disorders? Neuropathology. 2001b; 21:1–12. [PubMed: 11304036]

Armstrong RA, Lantos PL, Cairns NJ. Progressive supranuclear palsy (PSP: a quantitative study of the pathological changes in cortical and subcortical regions of eight cases. J Neural Transm. 2007a; 114:1569–1577. [PubMed: 17680229]

Armstrong RA, Lantos PL, Cairns NJ. Spatial topography of the neurofibrillary tangles in cortical and subcortical regions in progressive supranuclear palsy. Parkinson Rel Disord. 2007b; 13:50–54.

Armstrong RA, McKee AC, Stein TD, Alvarez VE, Cairns NJ. A quantitative study of tau pathology in 11 cases of chronic traumatic encephalopathy. Neuropathol Appl Neurobiol. 2016

Bell M, Ball M. Neuritic plaques and vessels of visual cortex in ageing and Alzheimer's dementia. Neurobiol Ageing. 1990; 11:359–370.

Crary JF, Trojanowski JQ, Schneider JA, Abisambra JF, El Abner, Alafuzoff I, Arnold SE, Attems J, Beach TG, Bigio EH, Cairns NJ, Dickson DW, Gearing M, Grinberg LT, Hof PR, Hyman BT, Jellinger K, Jicha GA, Kovacs GG, Knopman PS, Kofler J, Kukull WA, McKenzie IR, Masliah E, McKee A, Montine TJ, Murray ME, Neltner JH, Santa Maria I, Seeley WW, Serramo-Pozo A, Shelanski ML, Stein T, Takao M, Thal DR, Toledo JB, Troncoso J, Vonsattel JP, White CL, Wisniewski T, Woltzer RL, Yamada M, Nelson PT. Primary age-related tauopathy (PART): a common pathology associated with human aging. Acta Neuropathol. 2014; 128:755–766. [PubMed: 25348064]

De Lacoste M, White CL. The role of cortical connectivity in Alzheimer's disease pathogenesis: a review and model system. Neurobiol Aging. 1993; 14:1–16. [PubMed: 8450928]

Dickson DW. Neuropathology of non-Alzheimer degenerative disorders. Int J Clin Exp Pathol. 2009; 3:1–23. [PubMed: 19918325]

Geddes J, Vowles G, Nicoll J, Revesz T. Neuronal cytoskeletal changes are an early consequence of repetitive brain injury. Acta Neuropathol. 1999; 98:171–178. [PubMed: 10442557]

Goedert M, Clavaguera F, Tolnay M. The propagation of prion-like protein inclusions in neurodegenerative diseases. Trends Neurosci. 2010; 33:317–325. [PubMed: 20493564]

Goldstein LE, Fisher AM, Tagge CA, Zhang XL, Velisek L, Sullivan JA, Upreti C, Kracht JM, Ericsson M, Wojnarowicz MW, Goletani CJ, Maglakelidze GM, Casey M, Moncaster JA, Minaeva O, Moir MD, Nowinski CJ, Stern RA, Cantu RC, Geiling J, Blustajn JK, Wolozin BL, Ikezu T, Stein TD, Budson AE, Kowall NW, Chargin D, Sharon A, Samans S, Hall GF, Moss WC, Cleveland RO, Tanzi RE, Stanton PK, McKee AC. Chronic traumatic encephalopathy in blast-exposed military veterans and a blast neurotrauma mouse model. Sci Transl Med. 2012; 4:134ra60.

Graham DI, Gentleman SM, Lynch A, Roberts GW. Distribution of beta-amyloid protein in the brain following severe head-injury. Neuropath Appl Neurobiol. 1995; 21:27–34.

Hiorns RW, Neal JW, Pearson RCA, Powell TPS. Clustering of ipsilateral cortico-cortical projection neurons to area 7 in the rhesus monkey. Proc R Soc (Lond) B. 1991; 246:1–9.

Hyman BT, Phelps CH, Beach TG, Bigio EH, Cairns NJ, Carrillo MC, Dickson DW, Duyckaerts C, Frosch MP, Masliah E, Mirra SS, Nelson PT, Schneider JA, Thal DR, Thies B, Trojanowski JQ, Vinters HV, Montine TJ. National Institute on Aging-Alzheimer's Association guidelines for the neuropathologic assessment of Alzheimer's disease. Alzheimer Dement. 2012; 8:1–13.

Johnson VE, Stewart W, Smith DH. Widespread tau and amyloid-beta pathology many years after a single traumatic injury in humans. Brain Pathol. 2012; 22:142–149. [PubMed: 21714827]

Jordan BD. The clinical spectrum of sport-related traumatic brain injury. Nat Rev Neurol. 2013; 9:222–230. [PubMed: 23478462]

Josephs KA, Whitwell JL, Jack CR, Parisi JE, Dickson DW. Frontotemporal lobar degeneration without lobar atrophy. Arch Neurol. 2006; 63:1632–1638. [PubMed: 17101834]

Kawai M, Kalaria R, Harik S, Perry G. The relationship of amyloid plaques to cerebral capillaries in Alzheimer's disease. Am J Pathol. 1990; 137:1435–1446. [PubMed: 2260630]

Kieman PT, Montinegro PH, Solomon TM, McKee AC. Chronic traumatic encephalopathy: A neurodegenerative consequence of repetitive brain injury. Sem Neurol. 2015; 35:20–28.

Luthert P, Williams J. A quantitative study of the coincidence of blood vessels and A4 protein deposits in Alzheimer's disease. Neurosci Lett. 1991; 126:110–112. [PubMed: 1922919]

Maroon JC, Winkelman R, Bost J, Amos A, Mathyssek C, Miele V. Chronic traumatic encephalopathy in contact sports: a systematic review of all reported pathological cases. PLoS One. 2015; 10:e0117338. [PubMed: 25671598]

McKee AC, Stein TD, Nowinski CJ, Stern RA, Daneshvar DH, Alvarez VE, et al. The spectrum of disease in chronic traumatic encephalopathy. Brain. 2013; 136:43–64. [PubMed: 23208308]

McKee AC, Daneshvar DH, Alvarez VE, Stein TD. The neuropathology of sport. Acta Neuropathol. 2014; 127:29–51. [PubMed: 24366527]

McKee AC, Stein TD, Kieman PT, Alvarez VE. The neuropathology of chronic traumatic encephalopathy. Brain Pathol. 2015; 25:350–364. [PubMed: 25904048]

McKee AC, Cairns NJ, Dickson DW, Folkerth RD, Keene CD, Litvan I, Perl D, Stein TD, Vonsattel JP, Stewart W, Tripodis Y, Crary JF, Bienick KF, Dams-O'Connor K, Alverez VF, Gordon WA. The TBI, CTE Group. The first NINDS/NIBIB consensus meeting to define neuropathological criteria for the diagnosis of chronic traumatic encephalopathy. Acta Neuropathol. 2016; 131:75–86. [PubMed: 26667418]

Saing T, Dick M, Nelson PT, Kim RC, Cribbs DH, Head E. Frontal cortex neuropathology in dementia pugilistica. J Neurotrauma. 2012; 29:1054–1070. [PubMed: 22017610]

Schmidt M, Zhukareva V, Newell L, Lee V, Trojanoswki J. Tau isoform profile and phosphorylation state in dementia pugilistica recapitulate Alzheimer's disease. Acta Neuropathol. 2001; 101:518–524. [PubMed: 11484824]

Shetty AK, Mishra V, Kodali M, Hattiangady B. Blood brain barrier dysfunction and delayed neurological deficits in mild traumatic brain injury induced by blast shock waves. Front Cell Neurosci. 2014; 8:232. [PubMed: 25165433]

Stein TD, Alvarez VE, McKee AC. Chronic traumatic encephalopathy: a spectrum of neuropathological changes following repetitive brain trauma in athletes and military personnel. Alzheimer Res Ther. 2014; 6:4.

Stein TD, Montenigro PH, Alvarez VE, Xia W, Crary JF, Tripodis Y, Daneshvar DH, Mez J, Soloman T, Meng G, Kubilus CA, Cormier KA, Meng KA, Babcock K, Kiernan P, Murphy L, Nowiski CK, Martin B, Dixon D, Stern RA, Cantu RC, Kowall NW, McKee AC. Beta-amyloid deposition in chronic traumatic encephalopathy. Acta Neuropathol. 2015; 130:21–34. [PubMed: 25943889]

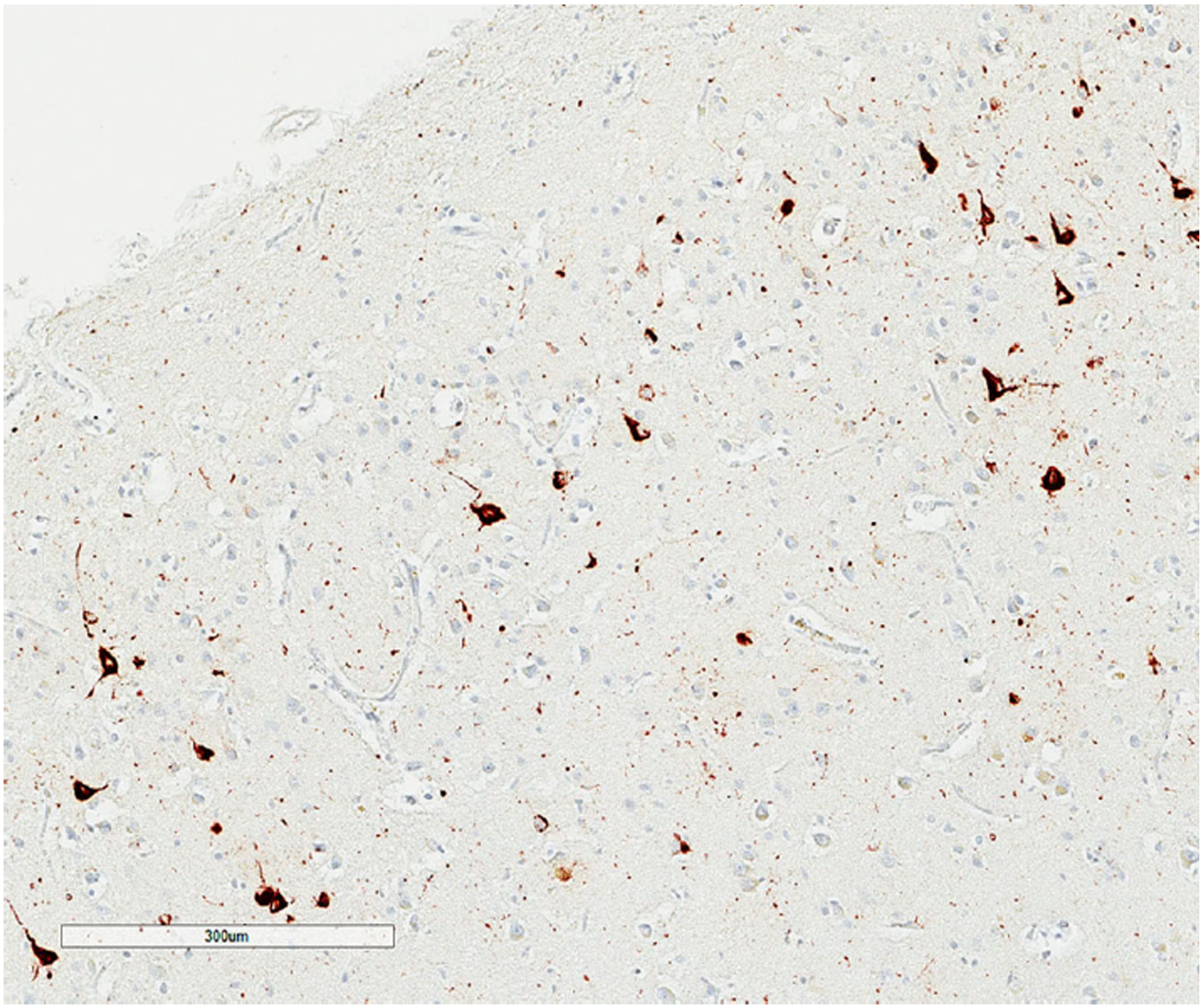

Fig. 1.

Tau-immunoreactive pathology at the temporal pole (TP) of a case of chronic traumatic encephalopathy (CTE) (Case A) showing clusters of neurofibrillary tangles (NFT) apparently regularly distributed parallel to the pia mater, dystrophic neurites (DN), and widespread dot-like grains (DLG), tau immunohistochemistry (AT8), and haematoxylin

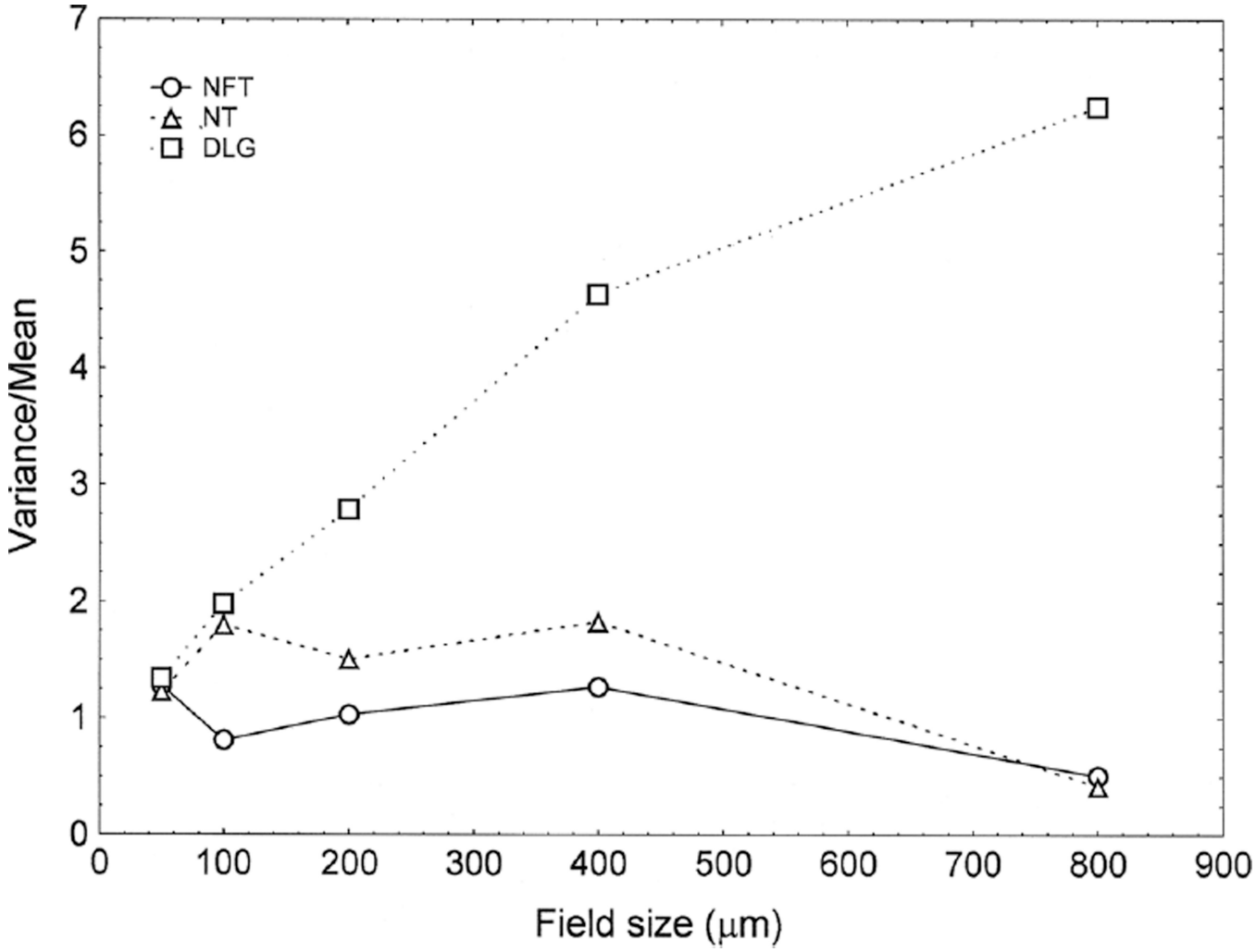

Fig. 2.

Examples of the spatial patterns exhibited by neurofibrillary tangles (*NFT*), dystrophic neurites (DN), and dot-like grains (*DLG*) in a case of chronic traumatic encephalopathy (CTE) (Case 6, entorhinal cortex)

Table 1

Demographic and neuropathology features of the cases, including National Institute on Aging–Alzheimer's association guidelines (NIA-AA), and 'ABC' scores (A = amyloid-beta, B = neurofibrillary tangles, C = neuritic plaques)

Case	Age[a]	Onset (years)	Trauma (years)	Career length (years)	Pathology	CTE stage	A	B	C
A	75	65	10/2	18	CTE, ADNC, HS, TDP-43	3	A3	B2	C1
B	70	66	10/1	11	CTE, ADNC, TDP-43	3	A0	B2	C0
C	60	55	1/1	26	CTE, HS, TDP-43	2	A0	B1	C0
D	65	56	–	19	CTE, ADNC, HS, TDP-43	4	A2	B2	C1
E	70	61	3/0	21	CTE, TDP-43, PART, AGD	3	A0	B1	C0
F	80	67	F	12	CTE, ADNC, HS, TDP-43	4	A2	B2	C0
G	80	38	–	18	CTE, ADNC, TDP-43	4	A3	B2	C1
H	65	55	50/1	17	CTE/PART	3	A0	B2	C0
I	70	61	10/1	19	CTE, ADNC, TDP-43	3	A2	B1	C1
J	60	54	25/1	21	CTE, ADNC, TDP-43	4	A3	B2	C0
K	70	45	F	20	CTE	4	A0	B2	C0
ADNC									
A	90	85	–	–	ADNC		A3	B2	C1
B	70	67	–	–	ADNC/TDP-43		A2	B2	C1
C	80	75	–	–	ADNC/AGD		A0	B1	C0
D	85	73	–	–	ADNC/VD		A3	B2	C1
E	90	81	–	–	ADNC/TDP-43		A2	B1	C1
F	70	56	–	–	ADNC		A1	B2	C1
G	70	62	–	–	ADNC		A3	B2	C1

F frequent, *ADNC* Alzheimer's disease neuropathologic change, *HS* hippocampal sclerosis, *TDP-43* transactive response (TAR) DNA-binding protein of 43 kDa, *PART* primary age-related tauopathy, *AGD* argyrophilic grain disease, *VD* vascular disease

[a] Age rounded to nearest 5-year age interval to protect subject identities

Table 2

Frequency of spatial patterns (*R* = random distribution, reg = regular or uniform distribution, reg clusters = regularly distributed clusters of inclusions) of the tau-immunoreactive neurofibrillary tangles (NFT), dystrophic neurites (DN), dot-like grains (DLG), astrocytic tangles (AT), and neuritic plaques (NP) in the cerebral cortex and hippocampus in 11 cases of chronic traumatic encephalopathy (CTE)

Pathology	Region	*R*	Reg	Reg clusters	Large clusters
NFT	Cortex	11	11	15 (6)	5
	Sub/HC/DG	5	7	13 (0)	7
NT	Cortex	3	1	26 (12)	10
	Sub/HC/DG	5	1	16 (0)	10
DLG	Cortex	2	0	21 (4)	20
	Sub/HC/DG	0	1	22 (0)	10
AT	Cortex	13	5	7 (6)	3
	Sub/HC/DG	4	0	1 (0)	0
NP	Cortex	2	0	1 (0)	0
	Sub/HC/DG	0	1	0	0

Figures in parentheses in column 5 indicate percentage of regions investigated in which cluster size was in the range 400–800 μm

Chi-square (χ^2) contingency tests: cortex vs Sub/HC/DG NFT $\chi^2 = 6.68$ (4DF, $P > 0.05$), NT $\chi^2 = 10.72$ (4DF, $P < 0.05$), DLG $\chi^2 = 21.25$ (4DF, $P < 0.001$), and AT $\chi^2 = 3.80$ (4DF, $P > 0.05$); among pathologies: cortex $\chi^2 = 71.20$ (16DF, $P < 0.001$) and HC/Sub $\chi^2 = 43.82$ (12DF, $P < 0.001$); among cases: CTE + CTE/PART compared with remaining cases NFT $\chi^2 = 0.59$ (3DF, $P > 0.05$), NT $\chi^2 = 4.73$ (3DF, $P > 0.05$), DLG $\chi^2 = 1.29$ (3DF, $P > 0.05$), and AT $\chi^2 = 4.68$ (3DF, $P > 0.05$); CTE cases with or without ADNC: NFT $\chi^2 = 3.53$ (3DF, $P > 0.05$), NT $\chi^2 = 2.94$ (3DF, $P > 0.05$), DLG $\chi^2 = 1.73$ (3DF, $P > 0.05$), and AT $\chi^2 = 1.73$ (3DF, $P > 0.05$); CTE cases with and without TDP-43 NFT $\chi^2 = 0.18$ (3DF, $P > 0.05$), NT $\chi^2 = 1.62$ (3DF, $P > 0.05$), DLG $\chi^2 = 1.35$ (3DF, $P > 0.05$), and AT $\chi^2 = 6.28$ (3DF, $P > 0.05$)

Table 3

Frequency of spatial patterns (*R* = random distribution, reg = regular or uniform distribution, reg clusters = regularly distributed clusters of inclusions) of the tau-immunoreactive neurofibrillary tangles (NFT) and neuritic plaques (NP) in the cerebral cortex and hippocampus in seven cases of Alzheimer's disease neuropathologic change (ADNC) without CTE

Pathology	Region	*R*	Reg	Reg clusters	Large clusters
NFT	Cortex	1	0	22 (12)	7
	Sub/HC/DG	3	0	9 (0)	1
NP	Cortex	1	1	12 (8)	12
	Sub/HC/DG	3	1	11 (0)	5

Figures in parentheses in column 5 indicate percentage of regions investigated in which cluster size was in the range 400–800 μm
Chi-square ($\chi 2$) contingency tests: CTE vs ADNC NFT $\chi 2 = 19.29$ (3DF, $P > 0.001$) and NP $\chi 2 = 9.80$ (3DF, $P < 0.05$)

Table 4

Frequency of significant spatial correlations between the tau-immunoreactive neurofibrillary tangles (NFT), dystrophic neurites (DN), dot-like grains (DLG), astrocytic tangles (AT), and neuritic plaques (NP) and larger blood vessel profiles (> 10 μm diameter) along the sides of gyri in the upper laminae of the cerebral cortex in 11 cases of chronic traumatic encephalopathy (CTE)

Correlation	NFT	NT	DLG	AT	NP
Positive	2	3	9	0	0
Negative	2	0	0	0	0
Not significant	40	41	35	37	5